NUMERICAL MODELLING OF QUANTUM DOTS

Abstract

A brief overview of Quantum Dots and their applications is presented. These pseudo-atoms or artificial atoms offer a vast range of practical applications since they are tunable with respect to their size, shape and composition. The essential ingredients for the theoretical study of their optical, thermal, electronic and transport properties is the energy spectra which can be obtained through numerical methods. One of the simplest and reliable methods is that based on the finite difference approach. The basic methodology for the same is mentioned. Some results for the energy levels of one-electron GaAs and InAs Quantum Dots are presented for spherical and cubical spatial confinements for different dot sizes. It is found that the effect of shape is independent of the type of semiconductor material of the Quantum Dot. The energy levels are higher in cubical confinement as compared to spherical confinement which can be explained to be due to the higher surface to volume ratio. Also it is found that energy values are higher for InAs QD than for GaAs QD which is due to the difference in the effective mass of the electron in the two different materials.

Keywords : Quantum Dots; numerical modelling; finite difference approach

Author

Shalini Lumb Talwar
Department of Physics
Maitreyi College
University of Delhi
Delhi, India.
slumb@maitreyi.du.ac.in

I. INTRODUCTION

The advanced semiconductor fabrication techniques led to the possibility of confining the bulk semiconductor material in one, two or three dimensions. Once the size of the nanomaterial becomes smaller than the bulk exciton Bohr radius in a particular dimension, quantum effects come into picture leading to the quantization of the energy levels in that dimension. This results in the well-known quantum structures called Quantum Wells, Quantum Wires and Quantum Dots (QDs). The field of Quantum nanostructures is well-studied [1-3]. Efros and Brus [3] present a detailed review covering the range of the theoretical and experimental information about the development and properties of QDs.

The confinement in different directions affects the density of states of the semiconductor material and hence the carrier concentration and energy distribution of carriers. In fact, in zero dimensional structures called QDs, the density of states is a delta function representing the discrete nature of the energy levels. Due to the quantization of the energy levels, such nanostructures can be considered to be just like atoms and are therefore called pseudo-atoms or artificial atoms. Such structures are known to have high surface to volume ratio which becomes nearly unity when all atoms are surface atoms. The electronic as well as thermodynamic properties are modified due to confinement. For example, the band gap in semiconductor nanomaterials become size-dependent. The melting point of metallic nanoparticles is comparatively low than the bulk material. With the decrease in the size of the QDs, the gap between the maximum of the valence band and the minimum of the conduction band increases thus increasing the band gap. This results in an increase in the excitation energy of the dot and the change in the color of the light emitted on de-excitation from red to blue or violet. This tunability of the band gap also provides control over the optical and electrical properties of QDs.

Typically, semiconductor QDs are 2-10 nm in size having diameter corresponding to 10-50 atoms and may include around 100-100000 atoms, although larger QDs of size 10-100 nm may be fabricated. A QD may be tuned to confine a precise number of electrons ranging from a single electron or a few electrons to several thousand electrons. With the aid of electrical contacts, electron transport through QDs is possible. The QD potential can be controlled by employing electrostatic gates. Simple QDs are synthesized from a single type of material, e.g., from silicon or germanium, so that they have uniform composition. The photophysical properties of QDs like luminescence can be increased by coating them with another higher band gap semiconducting material thus forming core-shell QDs, e.g., CdSe/CdZnS. The properties of QDs can also be tuned by adjusting their composition by alloying two semiconductor materials with different band gaps. For example, $Ag_2Se_xS_{1-x,}$ GaN–AlGaN and CdTeSe are alloyed QDs.

The optoelectronic properties of Quantum Dots are modified due to the presence of electric, magnetic and laser fields [4-6] or may be influenced due to different kind of potentials like Kratzer potential [7] and Hulthén-Yukawa potential [8]. The effect of size, shape and composition of the semiconductor nano structures on the band gap and electronic and optical properties is studied by several authors [9-17]. Higher-harmonic generation in different type of Quantum structures are also investigated [18-20]. Liang and Xie [11] investigate the influence of different shapes like circular, elliptic and triangular, on the optical absorption coefficients of QDs. Popescu et al. [14] mention that size is more important than

shape at the nanoscale.

One of the interesting and vital features in the study of QDs is the information about their electronic states. Several authors have studied the effect of size and shape on the energy levels of QDs [21-24]. Ngo et al. [21] have studied the electronic states of cuboidal, cylindrical, pyramidal, conical and lens-shaped InAs/GaAs QDs of different sizes. Kumar et al. [23] have considered how the anisotropy of shape and change in size modify the electronic structure of GaAs/AlGaAs quantum dots (QDs). Mantashian et al. [24] explore the electronic energy spectrum and probability densities for a varied range of shapes, viz., rectangular, spherical, cylindrical, ellipsoidal, spheroidal, conical QDs, QRs, nanotadpole QDs, and nanostars. The effect of dot size on the energy levels of a hydrogenic impurity in a spherical quantum dot is also investigated [25, 26]. Recently, the spectrum of excitons in a spherically confined quantum dot with linear potential and ionized donor hydrogenic impurity is evaluated in the presence of electric field along with the study of the linear and non-linear absorption coefficients [27].

The electronic states of QDs can be determined numerically or analytically. This chapter deals with the calculation of energy levels of InAs and GaAs spherical and cubical QDs. Although the shape of the QDs may deviate from an exact spherical to several other geometries like spheroidal, cylindrical, conical, lens-shaped or pyramidal, these are the simplest and most basic shapes that can be considered in order to get a glimpse of the electronic structure of QDs for different dot sizes and shapes. The basic methodology adopted for this numerical study is based on the finite-difference approach which is explained in detail. Section II highlights some of the important applications of QDs. This is followed by Section III giving the description of how the finite-difference method is employed to solve the radial Schrödinger equation to get the energy spectra. Some results are also discussed in this section. Section IV presents the summary.

II. APPLICATIONS

QDs have a wide range of applications ranging from LEDs, displays, photoconductors, photodetectors, biomedicine and catalysis [28]. QD-based devices are the base of the future generation technology. Quantum Dot-Based Light Emitting Diodes are set to provide a nice alternative to conventional LEDs. Studies to improve their efficiency are still underway [29, 30]. Controlled single-electron tunneling through QDs enables them to be used in single-electron transistors [31, 32]. These are based on the principle of Coulomb blockade and requires the charging energy, i.e., the amount of energy required to add one elementary charge to a QD, to be more than the thermal energy of the charge carriers so that they are not excited. The possibility of confinement of single electrons in controlled discrete energy states of semiconductor QDs makes them favorable for quantum computation [33, 34].

Since the semiconductor nonmaterials possess unique and tunable optoelectronic properties, they are suitable for many applications in the field of biomedicine. For example, various QDs on excitation by the same wavelength are seen to exhibit emission spectra depending on their size, shape, composition and doping. This fluorescent property of QDs makes them a favorable candidate for biomedical applications like targeted drug delivery, biosensors and probes for cellular imaging [35]. Tandale et al. [36] provide detailed

information about fluorescent quantum dots including various methods of synthesis and probable applications in biological field. Efforts are underway to synthesize materials of different sizes and morphologies to be employed in biomedical fields [37]. The rapidly evolving field of RNA nanotechnology is very promising for treatment of diseases. Sabzehmeidani and Kazemzad [38] discuss about QDs-based nanosensors for detection of antibodies.

III. NUMERICAL MODELLING

The electrons in the conduction band of a semiconductor are generally present near the minimum where the E-k diagram has a parabolic shape. Their dispersion relation is hence just like that for free electrons with their effective mass depending on the curvature of the E-k curve. In a similar manner, the holes which are present near the maximum of the valence band can be considered to have an effective mass in accordance with the curvature of the E-k diagram for the holes for that particular semiconductor. The determination of the energy spectra in the conduction as well as in the valence band of the QDs can therefore be considered to be a real life example of the usual 'particle in a box' problem. The present work is based on the same concept and involves the study of the effect of shape and size of the confining geometry on the electronic energy states for GaAs and InAs QDs. For the cubical confinement, the energy levels are well-known. For the spherical confinement, the energies are determined using nine-point finite-difference method.

1. **Time-Independent Radial Schrödinger Equation:** In order to get the electronic spectra, the time-independent Schrödinger equation is solved for the case of spherical confinement. The spherical boundary is taken into account by assuming that the form of the potential is $\mathbf{V(r) = 0}$ for $\mathbf{r < r_0}$ and $\mathbf{V(r)} = \infty$ for $\mathbf{r \geq r_0}$ so that the wave function vanishes beyond $\mathbf{r_0}$. This is known as hard wall or infinite spherical well confinement potential**.**

Due to the spherical symmetry, spherical coordinates may be employed to represent the Hamiltonian. In order to solve the Schrödinger equation, it is separated into radial and angular parts by the usual separation of variables technique. The wave functions are written as $\psi_{nlm}(r,\theta,\varphi) = R_{nl}(r)Y_{lm}(\theta,\varphi)$, where n, l and m are the principle, angular momentum and magnetic quantum numbers, respectively. $Y_{lm}(\theta,\varphi)$ are the spherical harmonics. The radial Schrödinger equation which needs to be solved is written in terms of the reduced radial wave function $U_{nl}(r) = rR_{nl}(r)$ as

$$-\frac{\hbar^2}{2m^*}\frac{d^2U_{nl}}{dr^2} + \left(V(r) + \frac{\hbar^2}{2m^*}\frac{l(l+1)}{r^2}\right)U_{nl} = E_{nl}U_{nl}. \quad (1)$$

In terms of the effective potential, $V_{eff}(r) = V(r) + \frac{\hbar^2}{2m^*}\frac{l(l+1)}{r^2}$, (1) takes the form

$$-\frac{\hbar^2}{2m^*}\frac{d^2U_{nl}}{dr^2} + V_{eff}(r)U_{nl} = E_{nl}U_{nl}. \quad (2)$$

For the hard wall confinement, this equation is solved only within the spherical boundary where $V(r)$ is zero.

Therefore the effective potential consists of only the centrifugal term $\frac{\hbar^2}{2m^*}\frac{l(l+1)}{r^2}$.

2. **Finite-Difference Method (FDM)**: The finite-difference method (FDM) is an approximate technique for solving partial differential equations with given boundary conditions and is very useful in solving many problems which cannot be solved analytically. FDM consists in discretizing the domain over which the equation is to be solved by forming a grid. For solving (2), the grid points are taken as $\boldsymbol{r_{i+1} = r_i + h}$, where $\boldsymbol{i = 1, 2, 3}$, ...N, so that the domain [$\boldsymbol{0}$,$\boldsymbol{r_0}$] is divided into $\boldsymbol{N}$ intervals. The number of grid points are adjusted so as to gain sufficient convergence.

The derivatives in the equation are replaced by finite difference approximations at each grid point. For example, the second order derivative in (2) may be replaced by the three-point central difference formula given by

$$f''(r_i) = \frac{f(r_i-h)-2f(r_i)+f(r_i+h)}{h^2} + O(h^2), \tag{3}$$

where $O(h^2)$ represents the order of error. Equation (2) is written as

$$-\frac{U_{nl}(r_i-h)-2U_{nl}(r_i)+U_{nl}(r_i+h)}{h^2} + \frac{l(l+1)}{r_i^2}U_{nl}(r_i) = \frac{2m^*E_{nl}}{\hbar^2}U_{nl}(r_i) \tag{4}$$

Putting $i = 1,2,3,\ldots$, a set of N linear simultaneous equations is formed. The terms corresponding to r_0 and r_{N+1} in the first and last equations are ignored. The system of equations is written in a matrix form as

$$-\frac{1}{h^2}\left\{\begin{bmatrix} -2 & 1 & 0 & 0 & \cdots & 0 & 0 & 0 & 0 \\ 1 & -2 & 1 & 0 & \cdots & 0 & 0 & 0 & 0 \\ 0 & 1 & -2 & 1 & \cdots & 0 & 0 & 0 & 0 \\ \vdots & \vdots & \vdots & \vdots & \ddots & \vdots & \vdots & \vdots & \vdots \\ 0 & 0 & 0 & 0 & \cdots & 1 & -2 & 1 & 0 \\ 0 & 0 & 0 & 0 & \cdots & 0 & 1 & -2 & 1 \\ 0 & 0 & 0 & 0 & \cdots & 0 & 0 & 1 & -2 \end{bmatrix} + l(l+1)\begin{bmatrix} 1/r_1^2 & 0 & 0 & 0 & \cdots & 0 & 0 & 0 & 0 \\ 0 & 1/r_2^2 & 0 & 0 & \cdots & 0 & 0 & 0 & 0 \\ 0 & 0 & 1/r_3^2 & 0 & \cdots & 0 & 0 & 0 & 0 \\ \vdots & \vdots & \vdots & \vdots & \ddots & \vdots & \vdots & \vdots & \vdots \\ 0 & 0 & 0 & 0 & \cdots & 0 & 1/r_{N-2}^2 & 0 & 0 \\ 0 & 0 & 0 & 0 & \cdots & 0 & 0 & 1/r_{N-1}^2 & 0 \\ 0 & 0 & 0 & 0 & \cdots & 0 & 0 & 0 & 1/r_N^2 \end{bmatrix}\right\}$$

$$\begin{bmatrix} U_{nl}(r_1) \\ U_{nl}(r_2) \\ U_{nl}(r_3) \\ \vdots \\ U_{nl}(r_{N-2}) \\ U_{nl}(r_{N-1}) \\ U_{nl}(r_N) \end{bmatrix} = \frac{2m^*E_{nl}}{\hbar^2}\begin{bmatrix} U_{nl}(r_1) \\ U_{nl}(r_2) \\ U_{nl}(r_3) \\ \vdots \\ U_{nl}(r_{N-2}) \\ U_{nl}(r_{N-1}) \\ U_{nl}(r_N) \end{bmatrix} \tag{5}$$

In order to avoid the singularity at the origin and to take the boundary condition into account, the first and last rows and columns are deleted and the problem reduces to solving a system of $N-2$ equations. Equation (5) is an eigenvalue problem involving (N-2) x (N-2) matrices, which may then be solved by the standard commands of programming platforms like MATLAB. It is solved using the atomic units where the mass of free electron, reduced Planck's constant and charge of an electron are taken as unity, i.e., $m_e = \hbar = e = 1$. The eigenvalues give the energy levels and the eigenvectors provide the corresponding $U_{nl}(r)$ and hence the wave functions. In order to enhance the accuracy, more accurate nine-point finite-difference method is employed in the present case.

3. **Results and Discussion:** First the energy levels for the simple case of an electron confined in a spherical cavity of radius $\boldsymbol{r_0}$ and a cubical cavity of length $\boldsymbol{L}$ are compared. The values of $\boldsymbol{r_0}$ and $\boldsymbol{L}$ are chosen so that they correspond to the same volume for the two geometries. Table 1 shows the first four energy levels for both the confining geometries for different dot sizes ranging from a radius of 5 nm to 15 nm for the spherical case and the corresponding side lengths of the cubical case. For the cubical QD, the first four distinct energy levels are considered. The energy increases for smaller dimensions in both the cases, which is the usual effect of confinement. It is observed that there is an increase of 15.45 percent in the ground state energy for cubical confinement with respect to the spherical confinement. The first, second and third excited states are similarly found to increase by 12.87, 2.91 and 5.83 percent, respectively. That is, different energy levels are affected to different extent but the ground state is affected the most.

Table 1: First four energy levels for spherical and cubical Quantum Dots of same volume as a function of the radius r_0 and length L, respectively

Spherical QD					**Cubical QD**				
$\boldsymbol{r_0}$ **(nm)**	$\boldsymbol{E_{00}}$ **(meV)**	$\boldsymbol{E_{01}}$ **(meV)**	$\boldsymbol{E_{02}}$ **(meV)**	$\boldsymbol{E_{10}}$ **(meV)**	$\boldsymbol{L}$ **(nm)**	$\boldsymbol{E_{111}}$ **(meV)**	$\boldsymbol{E_{112}}$ **(meV)**	$\boldsymbol{E_{122}}$ **(meV)**	$\boldsymbol{E_{113}}$ **(meV)**
5	15.04121	30.77054	50.62319	60.16485	8.06	17.36514	34.73028	52.09543	63.67219
6	10.44529	21.36843	35.15499	41.78114	9.67	12.05913	24.11825	36.17738	44.2168
7	7.67409	15.69925	25.82816	30.69635	11.28	8.85977	17.71953	26.5793	32.48581
8	5.87547	12.01974	19.77468	23.50189	12.9	6.78326	13.56652	20.34978	24.87195
9	4.64235	9.49708	15.62444	18.5694	14.51	5.35961	10.71922	16.07884	19.65191
10	3.7603	7.69263	12.6558	15.04121	16.12	4.34129	8.68257	13.02386	15.91805
11	3.10769	6.35755	10.45934	12.43075	17.73	3.58784	7.17568	10.76352	13.15541
12	2.61132	5.34211	8.78875	10.44529	19.34	3.01478	6.02956	9.04434	11.0542

13	2.22503	4.55185	7.48864	8.90013	20.96	2.56881	5.13762	7.70642	9.41896
14	1.91852	3.92481	6.45704	7.67409	22.57	2.21494	4.42988	6.64482	8.12145
15	1.67125	3.41895	5.6248	6.68498	24.18	1.92946	3.85892	5.78838	7.07469

The effect of the semiconductor environment is now taken into account by introducing the effective mass in the Schrödinger equation. The electronic states of an electron confined in GaAs and InAs QDs are determined for the two cavity shapes. The electron effective mass is taken to be $0.0665m_e$ for the GaAs QD and $0.04m_e$ for the InAs QD [ngo2006]. Figure 1 shows the first four energy levels for the two different semiconductor materials for different dot sizes for (a) a spherical QD of radius r_0 and (b) a cubical QD of length L.

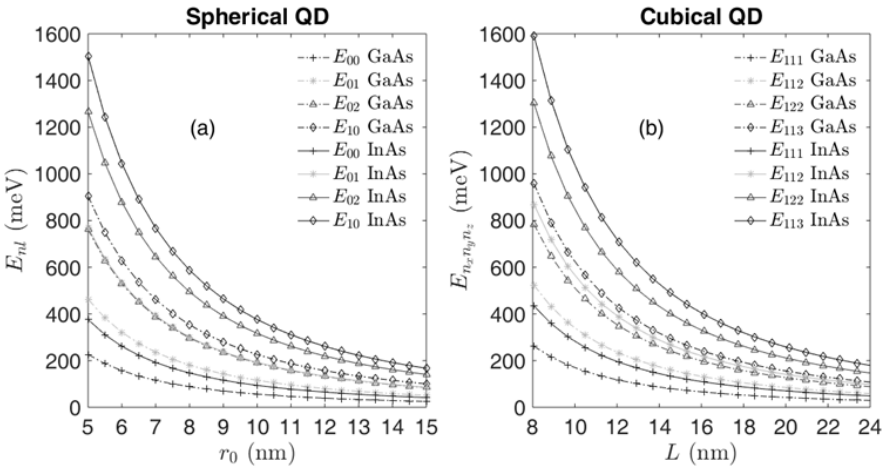

Figure 1: Variation of first four energy levels for GaAs and In As Quantum Dots for (a) a spherical QD of radius r_0 (b) a cubical QD of length L. For the cubical QD, the first four distinct energy levels are considered.

Analysis of the data shows that the percentage increase in the magnitude of energies with the change in confinement geometry from spherical to cubical is the same as for the corresponding case of an electron confined in these geometries as seen from the data given in Table 1. The increase in energy due to reduction in the size is of course evident. It may be mentioned that the shape and size effect is less apparent for comparatively higher dot sizes in absolute terms. Also, the percentage increase in energy for smaller dot sizes is more but the percentage increase in energy due to shape effect remains the same. This increase in the energies for the cubical case as compared to the spherical case is due to comparatively high surface to volume ratio.

It is also observed from Figure 1 that for InAs, the energy levels are placed higher as compared to those for GaAs. This can be easily explained on the basis of the nature of the E-k diagram since the effective mass of an electron in InAs is less than of that in GaAs. The effective mass is inversely related to the curvature of the E-k diagram. Hence a lower value of effective mass means higher curvature of the E-k curve which means higher energies for

lower k values.

IV. SUMMARY

The electronic energy spectra is determined for an electron in spherical and cubical confining geometries and also for an electron in GaAs and InAs spherical and cubical QDs. The energies are found to increase with confinement in all cases as expected. Also they are greater for cubical confinement than for spherical confinement although the dimensions of confining shapes are chosen such that the volume is held constant. It is observed that the shape effect is of similar nature for a single electron confined in a spherical or cubical geometry as for an electron confined to a semiconductor QD of the same dimensions. It is also found that the different energy levels are affected to different extent but the ground state is the most affected. Also, the energies are enhanced when the effective mass of the electron is lesser as for InAs in comparison to GaAs.

The knowledge of the dependence of the electronic spectra on the shape and material of the QDs provides information about how the electronic transition energies will be affected and is therefore important for understanding and predicting the behavior of QDs in important practical applications.

REFERENCES

[1] S.M. Reimann and M. Manninen, "Electronic structure of quantum dots", Rev. Mod. Phys., vol. 74, pp. 1283-1342, 2002.
[2] D. Bera, L. Qian, T.-K. Tseng, and P.H. Holloway, "Quantum Dots and Their Multimodal Applications: A Review", Materials, vol. 3, pp. 2260-2345, 2010.
[3] A.L. Efros and L.E. Brus, "Nanocrystal Quantum Dots: From Discovery to Modern Development", ACS Nano, vol. 15, pp. 6192-6210, 2021.
[4] T.G. Pedersen, "Stark effect in spherical quantum dots", Phy. Rev. A, vol. 99, pp. 063410, 2019.
[5] V. Prasad and P. Silotia, "Effect of laser radiation on optical properties of disk shaped quantum dot in magnetic fields" Physics Letters A, vol. 375, pp. 3910–3915, 2011.
[6] Y. Yakar, B. Çakır, and A. Özmen, "Magnetic field effects on oscillator strength, dipole polarizability and refractive index changes in spherical quantum dot", Chemical Physics Letters, vol. 708, pp. 138-145, 2018.
[7] K. Batra and V. Prasad, "Spherical quantum dot in Kratzer confining potential: study of linear and nonlinear optical absorption coefficients and refractive index changes", Eur. Phys. J. B, vol. 91, pp. 298, 2018.
[8] X. Li and C. Chang, "Nonlinear optical properties of GaAs/$Al_{\eta}Ga_{1-\eta}As$ quantum dots system with Hulthén-Yukawa potential", Optical Materials, vol. 131, pp. 112605, 2022.
[9] A. Schliwa, M. Winkelnkemper, and D. Bimberg, "Impact of size, shape, and composition on piezoelectric effects and electronic properties of In(Ga)As/GaAs quantum dots", Phys. Rev. B, vol. 76, pp. 205324, 2007.
[10] W.C. Yek, G. Gopir, and A.P. Othman, "Calculation of electronic properties of InAs/GaAs cubic, spherical and pyramidal Quantum Dots with finite difference method", Adv. Mat. Res., vol. 501, pp. 347-351, 2012.
[11] L. Liang and W. Xie, "Influence of the shape of quantum dots on their optical absorptions", Physica B, vol. 462, pp. 15-17, 2015.
[12] M. Singh, M. Goyal, and K. Devlal, "Size and shape effects on the band gap of semiconductor compound nanomaterials", J. Taibah Univ. Sci., vol. 12, pp. 470-475, 2018.
[13] Y. Liu, S. Bose, and W. Fan, "Effect of size and shape on electronic and optical properties of CdSe quantum dots", Optik, vol. 155, pp. 242-250, 2018.
[14] I. Popescu, M. Hristache, S.-S. Ciobanu, M.G. Barseghyan, J.A. Vinasco, A.L. Morales, A. Radu, and C.A. Duque, Comput. Mater. Sci., vol. 165, pp. 13-22, 2019.
[15] M. Goyal and M. Singh, "Size and shape dependence of optical properties of nanostructures", Applied

Physics A, vol. 126, pp. 176, 2020.
[16] S.H. Kim, M.T. Man, J.W. Lee, K.-D. Park, and H.S. Lee, "Influence of size and shape anisotropy on optical properties of CdSe Quantum Dots", Nanomaterials, vol. 10, pp. 1589, 2020.
[17] S. Hértilli, N. Yahyaoui, N. Zeiri, S. Saadaoui, and M. Said, "Energy levels and nonlinear optical properties of spheroid-shaped CdTe/ZnTe core/shell quantum dot", Optics & Laser Technology, vol. 155, pp. 108425, 2022.
[18] H. Bahramiyan and R. Khordad, "Optical properties of a GaAs pyramid Quantum Dot: second- and third harmonic generation", Int. J. Mod. Phys. B, vol. 28, pp. 1450053, 2014.
[19] V. V.Nautiyal and P. Silotia, "Second harmonic generation in a disk shaped quantum dot in the presence of spin-orbit interaction", Phys. Lett. A, vol. 382, pp. 2061-2068, 2018.
[20] M. Kirak and S. Yilmaz, "Third harmonic generation of spherical multilayered quantum dot: effects of quantum confinement, impurity, electric and magnetic fields", App. Phys. A, vol. 128, pp. 459, 2022.
[21] C.Y. Ngo, S.F. Yoon, W.J. Fan, and S.J. Chua, "Effects of size and shape on electronic states of quantum dots", Phys. Rev. B, vol. 74, pp. 245331, 2006.
[22] I. Saïdi, K. Sellami, M. Yahyaoui, C. Testelin, and K. Boujdaria, "Electron and hole energy levels in InAs/GaAs quantum dots: size and magnetic field effects" J. Appl. Phys., vol. 109, pp. 033703, 2011.
[23] D. Kumar, C.M.S. Negi, K.S. Gupta, and J. Kumar, "Shape and size dependent electronic properties of GaAs/AlGaAs Quantum Dots", Bonfring, Int. J. Power Syst. Integr. Circuits, vol. 2, pp. 23-26, 2012.
[24] G.A. Mantashian, P.A. Mantashyan, and D.B. Hayrapetyan, "Modeling of Quantum Dots with the finite element method", Computation, vol. 11, pp. 5, 2023.
[25] S.J. Liang and W.F. Xie, "The hydrostatic pressure and temperature effects on a hydrogenic impurity in a spherical quantum dot", Eur. Phys. J. B, vol. 81, pp. 79-84, 2011.
[26] J.-H. Yuan, L.-L. Wang, Z.-Y. Xiong, N. Chen, Z.-H. Zhang, and Y.-X. Zhao, "Hydrogenic impurity effect on the optical nonlinear absorption properties of spherical quantum dots with a parabolic potential", Eur. Phys. J. Plus, vol. 133, pp. 395, 2018.
[27] Varsha, M. Arora, M. Gambhir, and V. Prasad, "Anomalous Stark effect and optical properties of exciton in a quantum dot with linear potential under ionized donor hydrogenic impurity", Curr. App. Phys., vol. 48, pp. 17-28, 2023.
[28] M.A. Cotta (Ed.), "Quantum Dots and Their Applications: What Lies Ahead?", ACS Appl. Nano Mater., vol. 3, pp. 4920-4924, 2020.
[29] T. Lee, B. J. Kim, H. Lee, D. Hahm, W. K. Bae, J. Lim, and J. Kwak, "Bright and stable Quantum Dot Light-Emitting Diodes", Adv. Mat., vol. 34, pp. 2106276, 2022.
[30] J.H. Hwang, E. Seo, S. Park, K. Lee, D.H. Kim, S.H. Lee, Y.W. Kwon, J. Roh, J. Lim, and D. Lee, "All-solution-processed Quantum Dot Light-Emitting Diode using phosphomolybdic acid as hole injection layer", Materials, vol. 16, pp. 1371, 2023.
[31] R. Patel, Y. Agrawal, and R. Parekh, "Single-electron transistor: review in perspective of theory, modelling, design and fabrication", Microsyst. Technol., vol. 27, pp. 1863-1875, 2021.
[32] F. Abualnaja, W. He, K.-L. Chu, A. Andreev, M. Jones, and Z. Durrani, "Tunable hybrid silicon single-electron transistor–nanoscale field-effect transistor operating at room temperature", Appl. Phys. Lett., vol. 122, pp. 233504, 2023.
[33] D. Loss and D.P. DiVincenzo, "Quantum computation with quantum dots", Phys. Rev. A, vol. 57, pp. 120-126, 1998.
[34] X. Zhou, L. Zhai, and J. Liu, "Epitaxial quantum dots: a semiconductor launchpad for photonic quantum technologies", Photonics Insights, vol. 1, pp. R07, 2022.
[35] A.A.H. Abdellatif, M.A. Younis, M. Alsharidah, O.A. Rugaie, and H.M. Tawfeek, "Biomedical Applications of Quantum Dots: overview, challenges, and clinical potential", Int. J. Nanomed., vol. 17, 1951–1970, 2022.
[36] P. Tandale, N. Choudhary, J. Singh, A. Sharma, A. Shukla, P. Sriram, U. Soni, N. Singla, R. P. Barnwal, G. Singh , I. P. Kaur, and A. Suttee, "Fluorescent quantum dots: An insight on synthesis and potential biological application as drug carrier in cancer", Biochem. Biophys. Rep., vol. 26, pp. 100962, 2021.
[37] N. Babayevska, Ł. Przysiecka, I. Iatsunskyi, G. Nowaczyk, M. Jarek, E. Janiszewska, and S. Jurga, "ZnO size and shape effect on antibacterial activity and cytotoxicity profile", Sci. Rep., vol. 12, pp. 8148, 2022.
[38] M.M. Sabzehmeidani and M. Kazemzad, "Quantum dots based sensitive nanosensors for detection of antibiotics in natural products: A review", Sci. Total Environ., vol. 810, pp. 151997, 2022.

